Tohoku J. Exp. Med., 2024, **264**, 203-213

Association between NLRP3 Inflammasome and Tumor-Node-Metastasis Staging in Prostate Cancer: Immunohistochemical Studies of Prostate Needle Biopsy and Radical Prostatectomy Specimens

Toshiya Miyauchi,[1,2,3] Shintaro Narita,[4] Yuriko Saiki,[3,5,6] Yukitsugu Kudo-Asabe,[1] Akira Horii,[3] Shinichi Fukushige,[3,7] Tomonori Habuchi,[4] Hiroshi Nanjo[2] and Akiteru Goto[1]

[1]Department of Cellular and Organ Pathology, Graduate School of Medicine, Akita University, Akita, Akita, Japan
[2]Department of Clinical Pathology, Akita University Hospital, Akita, Akita, Japan
[3]Department of Molecular Pathology, Graduate School of Medicine, Tohoku University, Sendai, Miyagi, Japan
[4]Department of Urology, Graduate School of Medicine, Akita University, Akita, Japan
[5]Office of Medical Education, Graduate School of Medicine, Tohoku University, Sendai, Miyagi, Japan
[6]Department of Investigative Pathology, Graduate School of Medicine, Tohoku University, Sendai, Miyagi, Japan
[7]Department of Metabolism and Diabetes, Graduate School of Medicine, Tohoku University, Sendai, Miyagi, Japan

The pathological role of NLRP3 inflammasome in prostate cancer (PCa) remains unclear. This study aimed to elucidate the expression of its major components in PCa by immunohistochemistry and its clinicopathological significance. An immunohistochemical analysis of 184 prostate needle biopsy and 38 radical prostatectomy specimens from PCa revealed the expression status of NLRP3, PYCARD, and caspase-1, which form NLRP3 inflammasome. Furthermore, the association between the expression of these 3 proteins and the clinical parameters at diagnosis and operation was analyzed. In biopsy specimens, the Cochran-Armitage test demonstrated that the proportion of the high expression of NLRP3 ($P < 0.001$) and PYCARD ($P < 0.001$) in cancerous tissue tended to increase as the value of the Gleason Grade Group increased, and immunohistochemistry of NLRP3 and PYCARD helped to distinguish cancerous tissue from adjacent noncancerous tissue in some cases. Furthermore, a univariable logistic regression analysis revealed the high expression of NLRP3 to be associated with clinical T3–4 ($P = 0.0056$) and distant metastasis at diagnosis ($P = 0.011$), while the high expression of PYCARD was associated with clinical T3–4 ($P < 0.001$), regional lymph node metastasis ($P < 0.001$), and distant metastasis at diagnosis ($P < 0.001$). However, a multivariable logistic regression analysis showed no significant association. In prostatectomy specimens, no significant association existed between the expression of NLRP3 inflammasome and the clinical parameters at operation, partly due to the influence of neoadjuvant chemohormonal or hormone therapy. In conclusion, these results suggest that NLRP3 inflammasome may promote disease progression and metastasis in PCa, therefore immunohistochemistry of NLRP3 and PYCARD could be useful for diagnosing PCa accurately.

Keywords: immunohistochemistry; NLRP3 inflammasome; prostate cancer; PYCARD; tissue specimens
Tohoku J. Exp. Med., 2024 December, **264** (4), 203-213.
doi: 10.1620/tjem.2024.J074

Introduction

Prostate cancer (PCa) is the second most frequent cancer and fifth leading cause of cancer-related deaths among men worldwide (Bray et al. 2024). PCa is generally diagnosed by histopathological examination of ultrasound-guided prostate needle biopsy (Merriel et al. 2018). A histological examination can not only distinguish PCa from

Received June 27, 2024; revised and accepted July 23, 2024; J-STAGE Advance online publication August 1, 2024
Correspondence: Toshiya Miyauchi, Department of Cellular and Organ Pathology, Graduate School of Medicine, Akita University, 1-1-1 Hondo, Akita 010-8543, Japan.
e-mail: tmiyauchi@med.tohoku.ac.jp
©2024 Tohoku University Medical Press. This is an open-access article distributed under the terms of the Creative Commons Attribution-NonCommercial-NoDerivatives 4.0 International License (CC-BY-NC-ND 4.0). Anyone may download, reuse, copy, reprint, or distribute the article without modifications or adaptations for non-profit purposes if they cite the original authors and source properly.
https://creativecommons.org/licenses/by-nc-nd/4.0/

benign lesions but also evaluate the grade of PCa based on Gleason score (GS) (van Leenders et al. 2020). The Gleason Grade Group (GG) is a modified classification based on GS that more accurately reflects the prognosis: GG1 = GS ≤ 6, GG2 = GS 3 + 4, GG3 = GS 4 + 3, GG4 = GS 8, and GG5 = GS ≥ 9 (Pierorazio et al. 2013). Treatment options depend on prognostic factors, including the initial prostate-specific antigen (PSA) level, clinical tumor-node-metastasis (cTNM) stage, age, GS, and GG (Sekhoacha et al. 2022). Patients with localized lesions are offered active surveillance, radical prostatectomy, and radiotherapy, whereas those with advanced lesions are recommended chemotherapy or hormone therapy (Sekhoacha et al. 2022). Hormone therapy includes luteinizing hormone-releasing hormone (LHRH) agonists or antagonists, anti-androgens, and orchiectomy. Prostate needle biopsy and prostatectomy specimens should be analyzed to avoid selection bias, because patients who undergo prostatectomy tend to have localized lesions and are at low risk.

Inflammasomes are protein complexes that consist of a Nod-like receptor (NLR), apoptosis-associated speck-like protein containing a CARD (ASC), and caspase-1 (Moossavi et al. 2018; Hamarsheh and Zeiser 2020). NLRs are pattern recognition receptors that recognize pathogen- or danger-associated molecular patterns (PAMPs or DAMPs). Nod-like receptor protein 3 (NLRP3) is one of the most characterized NLRs and contains an N-terminal pyrin domain (PYC), central NACHT domain, and C-terminal leucine-rich repeat (LRR) domain. PYCARD, referred to as TMS1 or ASC, contains a PYD and a C-terminal caspase-recruitment domain (CARD). Procaspase-1 contains both caspase-1 and CARD domains. The NLRP3 inflammasome forms in the cytoplasm and mediates inflammatory responses via activation and secretion of the inflammatory cytokines IL-1β and IL-18, which contribute to the establishment of the tumor microenvironment.

The role of the NLRP3 inflammasome in cancer has recently attracted much attention. It remains controversial whether the NLRP3 inflammasome has a pro-tumorigenic or anti-tumorigenic function in oncogenesis; however, intensive *in vitro* and *in vivo* studies have indicated that the NLRP3 inflammasome could promote progression and migration in PCa (Xu et al. 2021), breast cancer (Guo et al. 2016), lung cancer (Wang et al. 2016b), and colon cancer (Wang et al. 2016a). Furthermore, studies examining clinical specimens suggest that high NLRP3 expression may be correlated with a poor prognosis in PCa (Xu et al. 2021), laryngeal squamous cell carcinoma (Xue et al. 2019), colorectal cancer (Shi et al. 2021), and pancreatic cancer (Zheng and Liu 2022).

Our previous study (Miyauchi et al. 2021) which examined 50 prostatectomy specimens by immunohistochemistry showed no significant association between the expression status of PYCARD and clinical parameters, including GG and PSA recurrence. This may be partly due to the patient characteristics of prostatectomy specimens, localized lesions, or the limited number of cases. To resolve these problems, it would be preferable to analyze patients with advanced lesions and to increase the number of cases. In addition to PYCARD, the expression status of other components of the NLRP3 inflammasome, NLRP3 and caspase-1, was also analyzed.

In this study, an immunohistochemical analysis of 184 biopsies and 38 prostatectomy specimens obtained from PCa revealed the expression status of NLRP3, PYCARD, and caspase-1, which form the NLRP3 inflammasome. Furthermore, the association between the expression status of NLRP3 inflammasome and clinical parameters at the diagnosis and operation was analyzed.

Materials and Methods

Tissue specimens

A total of 216 consecutive patients were diagnosed with PCa using needle biopsy at Akita University Hospital (Akita, Japan) between 2011 and 2015. The patients in this study did not overlap with those reported in our previous study (Miyauchi et al. 2021). All participants were racially Japanese. Biopsies are generally performed for patients with aberrant PSA values (4.0 ng/mL or more) and/or abnormal digital rectal examination findings. Of the 216 biopsy specimens, 15% (32/216) were excluded from the analysis because they were deeply cut for other immunohistochemical analyses or were missing. After excluding 32 missing specimens, 184 (85%) specimens were included in the analysis. None of the patients had received radiotherapy, chemohormonal therapy, or hormone therapy prior to the biopsy. A digital rectal examination, computed tomography, magnetic resonance imaging, and bone scintigraphy were performed to determine cTNM categories. The patients underwent the following treatments: radical prostatectomy (n = 39), radiotherapy (n = 67), hormone therapy with distant metastasis (n = 33), hormone therapy without distant metastasis (n = 31), and active surveillance (n = 12). Two patients were lost to follow-up after the histological diagnosis and clinical staging.

Of the 184 patients, 39 underwent radical prostatectomy at the Akita University Hospital. Prior to prostatectomy, 15% (6/39) of patients received chemohormonal therapy, 15% (6/39) received hormone therapy, and 69% (27/39) received no neoadjuvant therapy for PCa. Androgen deprivation therapy followed by docetaxel and estramustine phosphate was administered as a neoadjuvant chemohormonal therapy for 18 weeks, as reported in our previous study (Narita et al. 2019). No residual cancer was found in the prostatectomy specimens of 1 patient after hormone therapy. After excluding this patient, 38 prostatectomy specimens were analyzed.

Tissue specimens were evaluated using hematoxylin and eosin (HE) staining. The histopathological diagnosis was verified by pathologists authorized by the Japanese Society of Pathology (TM and HN), and staging was classi-

Table 1. Association between clinicopathological parameters and immunostaining of NLRP3, PYCARD, and caspase-1 in cancerous cells in biopsy specimens.

Characteristics	Total	Immunostaining of NLRP3		*P* value	Immunostaining of PYCARD		*P* value	Immunostaining of caspase-1		*P* value
		Positive	Negative		Positive	Negative		Positive	Negative	
Total	184	131	53		47	137		177	7	
Age at diagnosis (years),	72.1, 73	72.8, 74	70.6, 71		73.7, 75	71.6, 72		72.2, 73	70.7, 71	
mean, median, range	52-93	54-93	52-83		54-93	52-88		52-93	60-77	
PSA at diagnosis (ng/ml),	148.3, 11.1	197.2, 12.8	27.6, 8.7		195.4, 21.8	132.2, 10		153.5, 11.2	18.4, 9	
mean, median, range	2.1-6949.1	2.1-6949.1	3.6-627.4		2.1-2710.6	3.6-6949.1		2.1-6949.1	7.3-64.7	
Gleason Grade Group										
GG1	25	10	15		2	23		22	3	
GG2	59	34	25		5	54		59	0	
GG3	29	24	5		6	23		28	1	
GG4	29	25	4		13	16		28	1	
GG5	42	38	4	<0.001**	21	21	<0.001**	40	2	0.078
clinical T										
cT1–2	136	89	47		24	112		131	5	
cT3–4	48	42	6	0.0031*	23	25	<0.001**	46	2	1.00
clinical N										
cN0	157	108	49		32	125		151	6	
cN1	27	23	4	0.11	15	12	<0.001**	26	1	1.00
clinical M										
cM0	151	101	50		30	121		145	6	
cM1	33	30	3	0.0053*	17	16	<0.001**	32	1	1.00
clinical Stage										
cStage I–II	129	82	47		21	108		124	5	
cStage III–IV	55	49	6	<0.001**	26	29	<0.001**	53	2	1.00
Treatment										
prostatectomy	39	26	13		4	35		39	0	
radiotherapy	67	44	23		14	53		63	4	
hormone therapy										
with distant metastasis	33	30	3		17	16		32	1	
without distant metastasis	31	23	8		8	23		30	1	
active surveillance	12	7	5		3	9		11	1	
unknown	2	1	1		1	1		2	0	

*P < 0.05, **P< 0.001. GG, Gleason Grade Group.

fied according to the Union for International Cancer Control (UICC) TNM staging system (Brierley et al. 2017). At Akita University Hospital, 12 specimens were routinely obtained per prostate needle biopsy and divided into 2-4 formalin-fixed, paraffin-embedded (FFPE) blocks. A case-level GG for biopsy was assigned by global scoring, which evaluates all specimens with cancerous regions, and 1 FFPE block, which included a cancerous region with the assigned GG, was selected for the analysis per patient. The prostatectomy specimen was sectioned into FFPE blocks (thickness: 5 mm). A case-level GG for prostatectomy was assigned using global scoring, and 1 FFPE block, which included a cancerous region with the assigned GG, was analyzed. All neoplasms were glandular, and no squamous or neuroendocrine tumors were diagnosed. In prostatectomy specimens that have undergone either neoadjuvant chemohormonal or hormone therapy, GS was not evaluated in order to avoid any spurious upgrading due to the therapeutic effects. The clinical and histopathological characteristics of the patients are summarized in Tables 1 and 2. Written informed consent was obtained from all the patients. This study was approved by the Ethics Committee of Akita University Hospital (accession number 1034).

Immunohistochemistry

Sections of 2 μm in thickness were prepared, deparaffinized in xylene, and dehydrated in ethanol. After activation in a Cell Conditioning Solution (CC1, Ventana Medical Systems, Inc. Oro Valley, AZ, USA) at 98°C for 40 min and cooling to room temperature for 15 min, followed by

Table 2. Association between clinicopathological parameters and immunostaining of NLRP3, PYCARD, and caspase-1 in cancerous cells in prostatectomy specimens.

Characteristics	Total	Immunostaining of NLRP3		*P* value	Immunostaining of PYCARD		*P* value	Immunostaining of caspase-1		*P* value
		Positive	Negative		Positive	Negative		Positive	Negative	
Total	38	28	10		8	30		36	2	
Age at diagnosis (years),	67.5, 68	67.5, 68	67.5, 67.5		68.3, 67.5	67.3, 68		67.9, 68	60.5, 60.5	
mean, median, range	55-77	55-77	58-75		59-77	55-76		55-77	58-63	
PSA at diagnosis (ng/ml),	11.7, 8.05	10.9, 7.5	14.0, 9.0		12.3, 8.0	11.5, 8.1		11.7, 8.1	12.3, 12.3	
mean, median, range	2.1-57.0	4.1-54.4	2.1-57.0		2.1-47.7	4.1-57.0		2.1-57.0	5.6-18.9	
Gleason Grade Group										
GG2 without neoadjuvant therapy	12	7	5		0	12		11	1	
GG3 without neoadjuvant therapy	9	9	0		0	9		9	0	
GG4 without neoadjuvant therapy	6	5	1	0.065	2	4	0.043*	6	0	1.00
chemohormonal therapy	6	3	3		3	3		5	1	
hormone therapy	5	4	1		3	2		5	0	
pathological T										
pT2	28	20	8		6	22		27	1	
pT3	10	8	2	0.70	2	8	1.00	9	1	0.46
pathological N										
pN0	13	10	3		3	10		12	1	
pN1	2	1	1	0.48	1	1	0.48	2	0	1.00
pNX	23	17	6		4	19		22	1	
pathological Stage										
pStage II	28	20	8		6	22		27	1	
pStage III–IV	10	8	2	0.70	2	8	1.00	9	1	0.46
Extraprostatic extention										
negative	29	21	8		6	23		28	1	
positive	9	7	2	1.00	2	7	1.00	8	1	0.42
Resection margin										
negative	32	22	10		7	25		30	2	
positive	6	6	0	0.17	1	5	1.00	6	0	1.00
Lymphatic invasion										
negative	31	23	8		5	26		30	1	
positive	7	5	2	1.00	3	4	0.15	6	1	0.34
Vascular invasion										
negative	34	25	9		7	27		32	2	
positive	4	3	1	1.00	1	3	1.00	4	0	1.00
Perineural invasion										
negative	14	9	5		3	11		13	1	
positive	24	19	5	0.45	5	19	1.00	23	1	1.00
Seminal vesicle invasion										
negative	35	26	9		8	27		34	1	
positive	3	2	1	1.00	0	3	1.00	2	1	0.15

*P < 0.05, **P < 0.001. GG, Gleason Grade Group.

incubation in methanol with 0.3% H_2O_2 for 15 min to block endogenous peroxidase activity, the sections were incubated at room temperature for 30 min with rabbit anti-human NLRP3 primary antibody (Proteintech, Rosemont, IL, USA, polyclonal, cat 19771-1-AP, 1:200), rabbit anti-human TMS1/PYCARD antibody (EU107, polyclonal, 1:1000), which was generated previously (Stone et al. 2004), and rabbit anti-human Caspase-1 antibody (Proteintech,

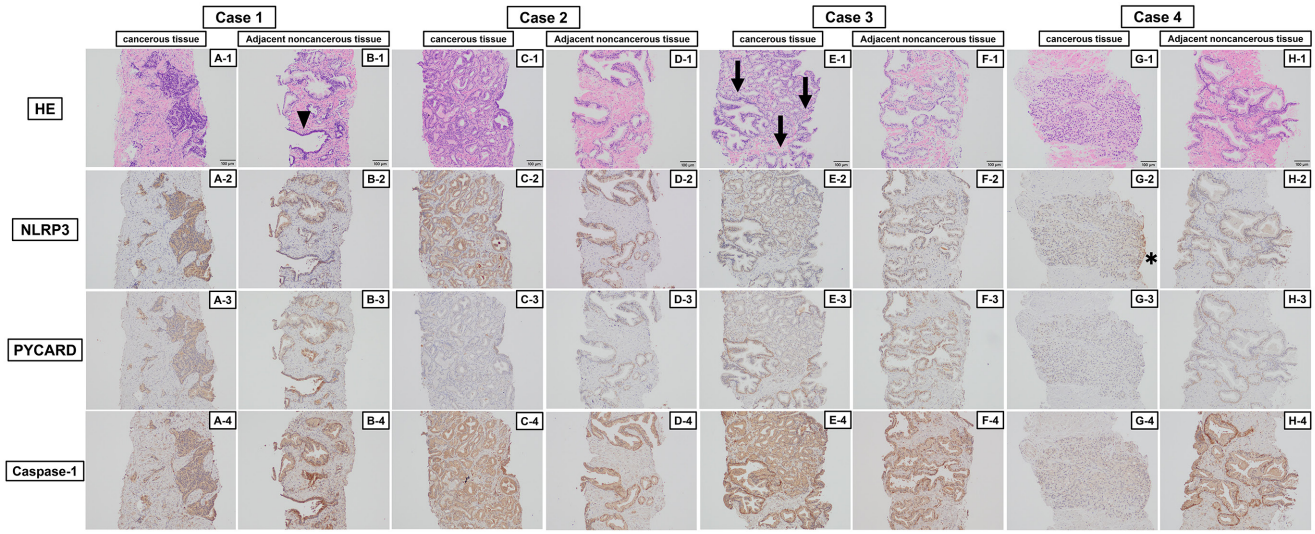

Fig. 1. Four representative expression patterns of NLRP3, PYCARD, and caspase-1 in cancerous tissues by immunohistochemical analysis.
For each case, cancerous tissue is shown in the left column (A, C, E, G). Adjacent noncancerous tissue is shown in the right column (B, D, F, H). Rows 1–4: HE, NLRP3, PYCARD, and caspase-1, respectively. Arrowhead in B-1 indicates basal cell hyperplasia. Arrows in E-1 indicate adjacent noncancerous cells. Asterisk in G-2 indicates nonspecific and negligible staining. Immunoreactivity was evaluated as follows: in Case 1, NLRP3 (+) / PYCARD (+) / caspase-1 (+) in cancerous cells, NLRP3 (−) / PYCARD (−) /caspase-1 (+) in adjacent secretory cells, and NLRP3 (−) / PYCARD (+) / caspase-1 (+) in adjacent basal cells; in Case 2, NLRP3 (+) / PYCARD (−) / caspase-1 (+) in cancerous cells, NLRP3 (−) / PYCARD (−) / caspase-1 (+) in adjacent secretory cells, and NLRP3 (+) / PYCARD (+) / caspase-1 (+) in adjacent basal cells; in Case 3, NLRP3 (−) / PYCARD (−) / caspase-1(+) in cancerous cells, NLRP3 (−) / PYCARD (−) / caspase-1 (+) in adjacent secretory cells, and NLRP3 (−) / PYCARD (+) / caspase-1 (+) in adjacent basal cells; in Case 4, NLRP3 (−) / PYCARD (−) / caspase-1 (−) in cancerous cells, NLRP3 (−) / PYCARD (−) / caspase-1 (+) in adjacent secretory cells, and NLRP3(−) / PYCARD (+) / caspase-1 (+) in adjacent basal cells.

Rosemont, IL, USA, polyclonal, cat 22915-1-AP, 1:500). A Histofine SAB-PO(R) kit (Nichirei Biosciences Inc., Chuo-ku, Tokyo, Japan) was used for staining NLRP3 and TMS1/PYCARD antibodies, while a Histofine Simple Stain MAX-PO(MULTI) kit (Nichirei Biosciences Inc., Chuo-ku, Tokyo, Japan) was used for staining caspase-1 antibody. Staining was performed according to the manufacturers' instructions. The sections were stained with DAB (Agilent Technologies, Inc., Santa Clara, CA, USA). As a negative control for the Histofine SAB-PO(R) and MAX-PO(MULTI) kits, the procedure was performed without adding the primary antibody.

Assessment of Immunohistochemistry

Immunoreactivity was evaluated by 3 pathologists authorized by the Japanese Society of Pathology (T.M., Y.S. and A.G.), without any information about the patients. The following criteria were used to evaluate the expression status of NLRP3, PYCARD, and caspase-1 in cancerous, adjacent secretory, and adjacent basal cells, respectively. The staining intensity in the cytoplasm was classified as no (0), weak (1+), moderate (2+), or strong (3+), as shown in Supplementary Fig. S1 Staining in the nucleus or cytomembranes was not evaluated. Specimens showing moderate (2+) or strong (3+) staining with more than 30% of the whole cells were defined as positive (+), while the others were defined as negative (−). Discordance was resolved by joint discussion among T.M., Y.S. and A.G.

Clinical parameters

The GG level, PSA at the diagnosis, and TNM stage were analyzed. Prognoses including PSA recurrence and survival rates were not analyzed for the following reasons: 1) 10s of patients were sent to other hospitals within 3 years of the diagnosis or treatment, and long-term follow-up was missed; and 2) patients were categorized into several groups due to the various treatment options for PCa (the prostatectomy group [n = 39] was categorized into prostatectomy with [n = 12] or without [n = 27] neoadjuvant therapy; the radiotherapy group [RT; n = 67] was categorized into 3-dimensional conformal radiation therapy [n = 35], intensity-modulated RT [n = 13], proton beam RT [n = 4], heavy particle RT [n = 2], and brachytherapy [n = 13]). Therefore, clinical information obtained at the diagnosis was analyzed, and prognoses were not analyzed.

Statistical analysis

Fisher's exact test was used to determine the association between clinical parameters at the diagnosis and at the operation and immunostaining for NLRP3, PYCARD, and caspase-1. The Cochran-Armitage test was utilized to assess any trends in the association between GG and the proportion of the NLRP3 inflammasome expression. Univariable and multivariable logistic regression analyses

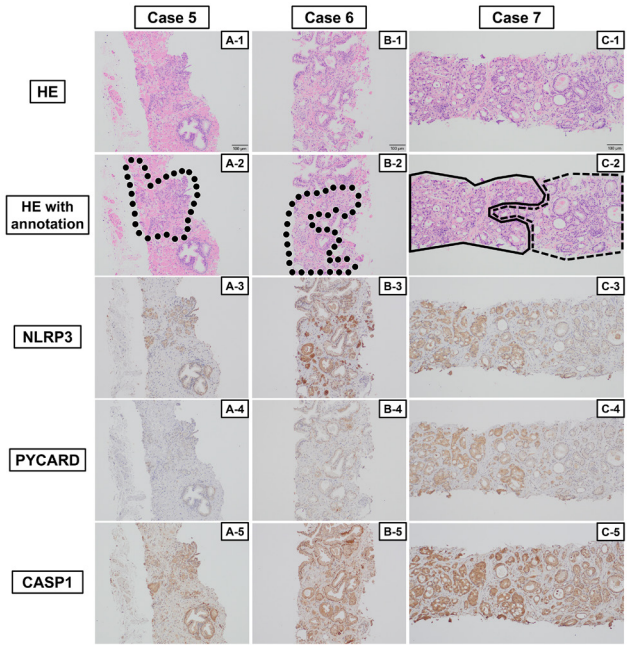

Fig. 2. Representative results of HE staining and immunohistochemical staining of 2 patients in which NLRP3 was useful for distinguishing cancerous tissue from adjacent noncancerous tissue and of 1 patient in which NLRP3 and PYCARD helped to discern the difference between the Gleason patterns.
Case 5 is shown in the left column (A). Case 6 is shown in the middle column (B). Case 7 is shown in the right column (C). Rows 1–5: HE, HE with annotation, NLRP3, PYCARD, and caspase-1, respectively. The annotation is as follows: cancerous tissue is surrounded by a dotted line in Cases 5 and 6; Gleason pattern 4 is surrounded by a solid line in Case 7; and Gleason pattern 3 is surrounded by a dashed line in Case 7.

were used to determine the association between cTNM categories and clinicopathological parameters, including the NLRP3 inflammasome expression status in biopsy specimens. The odds ratio of each variable was computed along with 95% confidence intervals (CIs). P values of < 0.05 were considered to indicate statistical significance. All analyses were performed using R version 4.4.0 (The R Foundation, Vienna, Austria).

Results

Immunohistochemical analysis of NLRP3, PYCARD, and caspase-1 at prostate needle biopsy specimens

Table 1 shows the expression status of NLRP3, PYCARD, and caspase-1 in cancerous cells obtained from biopsy specimens. The specimens were classified according to 4 expression patterns: NLRP3 (+) / PYCARD (+) / caspase-1 (+), NLRP3 (+) / PYCARD (−) / caspase-1 (+), NLRP3 (−) / PYCARD (−) / caspase-1 (+), and NLRP3 (−) / PYCARD (−) / caspase-1 (−). All PYCARD-positive specimens expressed NLRP3 and caspase-1, and all NLRP3-positive specimens expressed caspase-1. Representative results of the immunohistochemical analysis of the 3 proteins from the 4 patients are shown in Fig. 1. In Case 3, PYCARD helped to distinguish cancerous regions from adjacent noncancerous regions by identifying the presence or absence of basal cells. The Cochran-Armitage test demonstrated that the proportion of the high expression of NLRP3 ($P < 0.001$) and PYCARD ($P < 0.001$) tended to increase as the value of GG increased, while no significant trend was observed between GG and the expression status of caspase-1 ($P = 0.75$).

Of the 184 specimens, adjacent secretory and basal cells were not found in 10% (19/184) and 3.8% (7/184), respectively. Adjacent secretory cells were positive for NLRP3 (17%, 28/165), PYCARD (3.0%, 5/165), and caspase-1 (98%, 162/165). Adjacent basal cells were positive for NLRP3 (22%, 39/177), PYCARD (99%, 176/177), and caspase-1 (100%, 177/177).

Fig. 2 shows representative results of the immunohistochemical analysis, in which NLRP3 and PYCARD were useful for distinguishing cancerous tissue from adjacent noncancerous tissue and discerning the difference between the Gleason patterns. In Cases 5 and 6, NLRP3 was positive in cancerous cells but negative in adjacent noncancerous cells. In Case 7, NLRP3 and PYCARD were positive in cancerous cells with Gleason pattern 4 but negative in those with Gleason pattern 3.

Negative control slides showed negligible staining caused by endogenous peroxidase and biotin activities (Supplementary Fig. S2).

Immunohistochemical analysis of NLRP3, PYCARD, and caspase-1 at prostatectomy specimens

Table 2 shows the expression status of NLRP3, PYCARD, and caspase-1 in cancerous cells in prostatectomy specimens. Among the patients managed without neoadjuvant therapy, the Cochran-Armitage test showed that the proportion of the high expression of PYCARD ($P = 0.022$) in cancerous tissue tended to increase as the value of GG increased, while no significant trend was observed between GG and the expression status of NLRP3 ($P = 0.12$) and caspase-1 ($P = 0.31$). In addition to the 4 patterns of expression status of the 3 proteins acknowledged in the biopsy specimens, NLRP3 (−) / PYCARD (+) / caspase-1 (+) was acknowledged in 1 prostatectomy specimen from a patient who received neoadjuvant chemohormonal therapy. The supplementary tables show the comparison between the biopsy and corresponding prostatectomy specimens for cancerous cells (Supplementary Table S1), for specimens from patients managed without neoadjuvant therapy (Supplementary Table S2), for specimens from patients who received neoadjuvant chemohormonal therapy (Supplementary Table S3), and for specimens from patients who received neoadjuvant hormone therapy (Supplementary Table S4). Discordance between the specimens in the expression status of NLRP3 inflammasome components occurred when the specimens showed a differ-

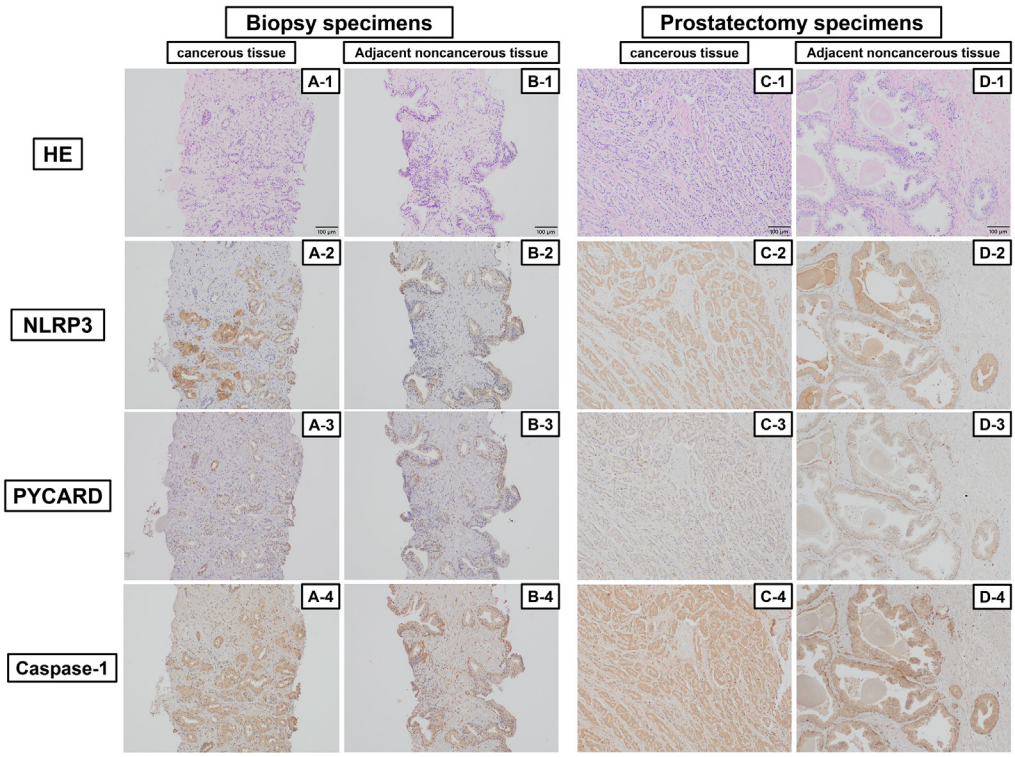

Fig. 3. Representative results of HE staining and immunohistochemical staining of biopsy and corresponding prostatectomy specimens from the same patient managed without neoadjuvant therapy.
Biopsy specimens are shown in the 2 left columns (A, B) and prostatectomy specimens are shown in the 2 right columns (C, D). Cancerous tissue is shown in the left column (A, C) and adjacent noncancerous tissue is shown in the right column (B, D) for each specimen. Rows 1–4: HE, NLRP3, PYCARD, and caspase-1, respectively. Immunoreactivity was evaluated as follows: in biopsy specimens, NLRP3 (+) / PYCARD (−) / caspase-1 (+) in cancerous cells, NLRP3 (−) / PYCARD (−) / caspase-1 (+) in adjacent secretory cells, and NLRP3 (−) / PYCARD (+) / caspase-1 (+) in adjacent basal cells; in prostatectomy specimens, NLRP3 (+) / PYCARD (−) / caspase-1 (+) in cancerous cells, NLRP3 (+) / PYCARD (−) / caspase-1 (+) in adjacent secretory cells, and NLRP3 (+) / PYCARD (+) / caspase-1 (+) in adjacent basal cells.

ent GG or when neoadjuvant chemohormonal or hormone therapy was administered after the biopsy.

Fig. 3 and 4 show representative results of the immunohistochemical analysis to detect the 3 proteins in biopsy specimens and corresponding prostatectomy specimens from patients managed without neoadjuvant therapy (Fig. 3) or with neoadjuvant hormone therapy (Fig. 4).

Of the 38 prostatectomy specimens, adjacent secretory cells were positive for NLRP3 in 100% (38/38), PYCARD in 34% (13/38), and caspase-1 in 100% (38/38), respectively. Adjacent basal cells were positive for NLRP3 (82%, 31/38), PYCARD (100%, 38/38), and caspase-1 (100%, 38/38).

Association between clinical parameters at the diagnosis and the expression status of NLRP3, PYCARD, and caspase-1 in biopsy specimens

Fisher's exact test revealed the following association: NLRP3 was more frequently positive in patients with cT3–4 and distant metastasis at the time of the diagnosis (cM1) than in those without; PYCARD was more frequently positive in patients with cT3–4, regional lymph node metastasis at the diagnosis (cN1), and cM1 than in those without. Although not statistically significant, NLRP3 was more frequently positive in patients with cN1 ($P = 0.11$). There was no significant association between the caspase-1 levels and clinical parameters at the diagnosis. Representative results of the analysis of the expression status of the 3 proteins and bone scintigraphy from 2 patients (with and without multiple bone metastases) are shown in Supplementary Fig. S3.

The univariable and multivariable logistic regression analyses are presented in Table 3. Although the multivariable logistic regression analysis showed no significant association between the expression status of NLRP3 inflammasome components and cTNM categories, the univariable logistic regression analysis revealed that the high expression of NLRP3 was associated with cT3–4, cM1, and cStage III–IV, and that the high expression of PYCARD was associated with cT3–4, cN1, cM1, and cStage III–IV.

Discussion

In this study, the immunohistochemical analysis of 184 biopsy specimens from PCa patients revealed that the proportion of the high expression of NLRP3 ($P < 0.001$) and PYCARD ($P < 0.001$) tended to increase as the value of GG

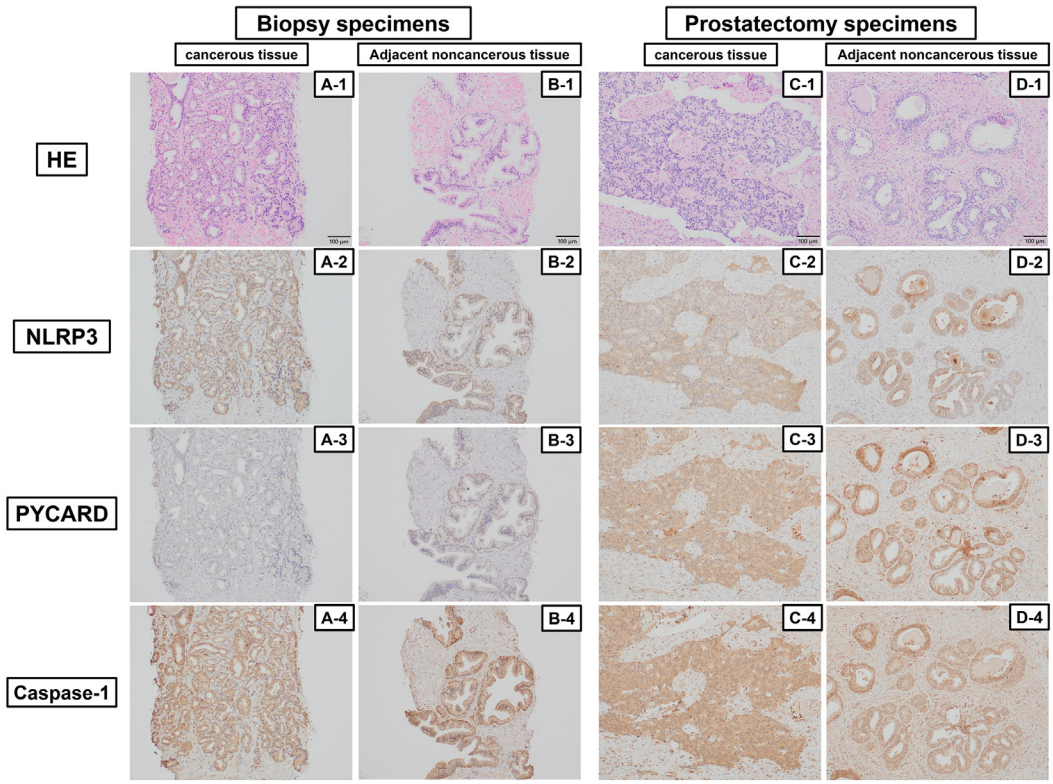

Fig. 4. Representative results of HE staining and immunohistochemical staining of biopsy and corresponding prostatectomy specimens from the same patient with neoadjuvant hormone therapy.
Biopsy specimens are shown in the 2 left columns (A, B) and prostatectomy specimens are shown in the 2 right columns (C, D). Cancerous tissue is shown in the left column (A, C) and adjacent noncancerous tissue is shown in the right column (B, D) for each specimen. Rows 1–4: HE, NLRP3, PYCARD, and caspase-1, respectively. Immunoreactivity was evaluated as follows: in biopsy specimens, NLRP3 (+) / PYCARD (-) / caspase-1 (+) in cancerous cells, NLRP3 (+) / PYCARD (-) / caspase-1 (+) in adjacent secretory cells, and NLRP3 (-) / PYCARD (+) / caspase-1 (+) in adjacent basal cells; in prostatectomy specimens, NLRP3 (+) / PYCARD (+) / caspase-1 (+) in cancerous cells, NLRP3 (+) / PYCARD (+) / caspase-1 (+) in adjacent secretory cells, and NLRP3 (+) / PYCARD (+) / caspase-1 (+) in adjacent basal cells.

increased. A univariable logistic regression analysis showed that the high expression of NLRP3 and PYCARD in biopsy specimens was associated with higher cTNM categories. In prostatectomy specimens, there was no significant association between the expression status of NLRP3 inflammasome and clinical parameters at the operation, partly due to the influence of neoadjuvant chemohormonal or hormone therapy. Furthermore, NLRP3 and PYCARD were useful for distinguishing cancerous regions from adjacent noncancerous regions in some biopsy specimens.

Studies examining the role of the NLRP3 inflammasome in PCa are limited. Two previous immunohistochemical studies (Xu et al. 2021; Karan et al. 2017) have shown controversial results. One study (Xu et al. 2021) which investigated 30 prostatectomy specimens obtained from PCa revealed that the high expression of NLRP3 in PCa was correlated with high pathological TNM stage and lymph node metastasis, and indicated that the expression of NLRP3 in cancerous tissue was higher than that in adjacent noncancerous tissue. Another study (Karan et al. 2017) which investigated 19 biopsy specimens of PCa showed heterogeneous NLRP3 staining in prostate tissue and no difference between cancerous and adjacent noncancerous tissues. Both studies focused on the expression status of NLRP3 but did not examine the expression status of PYCARD. Our results agreed with the former in the association between the high expression of NLRP3 and high TNM staging, and the latter in heterogeneous staining of NLRP3 in prostate tissue. As for heterogeneous staining, our results showed a remarkable feature of staining in Case 7 (Fig. 2): in cancerous tissue obtained from 1 patient, Gleason pattern 4 showed the high expression of NLRP3, whereas Gleason pattern 3 showed the low expression of NLRP3. Although heterogeneous staining may make immunohistochemistry rather difficult to evaluate, our method of assessment described in the Materials and Methods could distinguish the high expression of NLRP3 from the low expression of NLRP3 in prostate tissue. However, it is necessary to carefully evaluate a small amount of cancerous tissue because a biopsy specimen is only a part of the whole lesion.

The present study was associated with several limitations. This study failed to examine the mechanisms through which NLRP3 inflammasomes are involved in the progres-

Table 3. Univariable and multivariable logistic regression analyses of the association between cTNM categories and clinicopathological parameters in biopsy specimens.

	clinical T category				clinical N category			
	Univariable analysis		Multivariable analysis		Univariable analysis		Multivariable analysis	
	OR(95% CI)	*P* value	OR(95% CI)	*P* value	OR(95% CI)	*P* value	OR(95% CI)	*P* value
PSA at diagnosis (ng/ml)								
≤20	reference		reference		reference		reference	
>20	26.60 (11.23-63.00)	<0.001**	14.56 (6.00-37.88)	<0.001**	16.53 (5.82-46.97)	<0.001**	8.24 (2.52-26.91)	<0.001**
Gleason Grade Group								
GG1-3	reference		reference		reference		reference	
GG4-5	14.08 (6.17-32.17)	<0.001**	4.10 (1.47-11.45)	0.0071*	13.06 (4.28-39.81)	<0.001**	3.95 (1.01-15.39)	0.048*
NLRP3								
negative	reference		reference		reference		reference	
positive	3.70 (1.47-9.33)	0.0056*	1.62 (0.39-6.69)	0.50	2.61 (0.86-7.95)	0.092	0.64 (0.13-3.14)	0.58
PYCARD								
negative	reference		reference		reference		reference	
positive	4.29 (2.09-8.80)	<0.001**	1.71 (0.59-4.93)	0.32	4.88 (2.08-11.45)	<0.001**	2.40 (0.80-7.22)	0.12
caspase-1								
negative	reference		reference		reference		reference	
positive	0.88 (0.16-4.68)	0.88	0.23 (0.020-2.54)	0.23	1.03 (0.12-8.94)	0.98	0.63 (0.036-10.79)	0.75

	clinical M category				clinical Stage			
	Univariable analysis		Multivariable analysis		Univariable analysis		Multivariable analysis	
	OR(95% CI)	*P* value	OR(95% CI)	*P* value	OR(95% CI)	*P* value	OR(95% CI)	*P* value
PSA at diagnosis (ng/ml)								
≤20	reference		reference		reference		reference	
>20	12.60 (5.17-30.72)	<0.001**	4.48 (1.64-12.20)	0.0034*	28.83 (12.37-67.17)	<0.001**	15.78 (6.15-40.44)	<0.001**
Gleason Grade Group								
GG1-3	reference		reference		reference		reference	
GG4-5	26.83 (7.77-92.69)	<0.001**	11.01 (2.81-43.19)	<0.001**	15.11 (6.89-33.13)	<0.001**	4.53 (1.70-12.06)	0.0025*
NLRP3								
negative	reference		reference		reference		reference	
positive	4.95 (1.44-17.01)	0.011*	1.87 (0.33-10.79)	0.48	4.68 (1.86-11.75)	0.0010*	2.49 (0.60-10.29)	0.21
PYCARD								
negative	reference		reference		reference		reference	
positive	4.29 (1.94-9.45)	<0.001**	1.31 (0.48-3.58)	0.60	4.61 (2.28-9.34)	<0.001**	1.73 (0.60-5.02)	0.31
caspase-1								
negative	reference		reference		reference		reference	
positive	1.32 (0.15-11.38)	0.80	0.56 (0.030-10.57)	0.70	1.07 (0.20-5.68)	0.94	0.22 (0.019-2.59)	0.23

*P < 0.05, **P < 0.001. OR, odds ratio; 95% CI, 95% confidence interval; GG, Gleason Grade Group.

sion and metastasis of cancer. Recent *in vitro* or *in vivo* studies investigating the roles of NLRP3 inflammasomes in some cancers could support and reinforce this study: NLRP3 inflammasome may promote proliferation and migration via the activation of caspase-1 in PCa (Xu et al. 2021); regulation of epithelial–mesenchymal transition in colorectal cancer (Shao et al. 2020); elevation of the IL-1β expression in oral squamous cell carcinoma (Wang et al. 2018); and enhancement of phosphorylation of Akt, ERK1/2, and cAMP response element binding protein in lung cancer (Wang et al. 2016b).

A possible explanation for the association between the high expression of the NLRP3 inflammasome and high TNM stage is that its downstream cytokines IL-1β/IL-18 could contribute to the tumor microenvironment, which promotes the development and progression of cancer. *In vitro* and *in vivo* studies have indicated that the expression of IL-1β promoted bone metastasis in PCa (Shahriari et al. 2017; DiNatale at al. 2022). Serum IL-18 levels in PCa patients with cT3-4 were elevated in comparison to those with cT2 (Dwivedi et al. 2011). The evaluation of prostatectomy specimens in the present study revealed no statistically significant association between the expression status of the NLRP3 inflammasome and lymphovascular or perineural invasion that could be correlated with the tumor microenvironment. This may be partly due to the change in the NLRP3 inflammasome expression status caused by neoadjuvant chemohormonal or hormone therapy and may also be partly due to the small number of prostatectomy specimens obtained from the patients managed without neoadjuvant therapy. Therefore, further studies are required to examine the association between the NLRP3 inflammasome expression status in specimens and serum IL-1β/IL-18 levels in PCa, as well as to increase the number of prostatectomy specimens obtained from patients managed without neoadjuvant therapy.

In conclusion, this study suggests that the NLRP3 inflammasome may promote progression and metastasis in PCa, and that immunohistochemical staining of NLRP3 and PYCARD could be useful for the accurate diagnosis of PCa in biopsy specimens.

Acknowledgments

This work was supported by a Grant-in-Aid (Grant # 19K07454) from the Japan Society for the Promotion of Science (JSPS). We would like to thank Prof. Paula M. Vertino (University of Rochester Medical Center, Rochester, NY, USA) for providing us with the rabbit anti-human TMS1/PYCARD antibody (EU107, polyclonal) and Mr. Brian Quinn (Editor-in-Chief, Japan Medical Communication, Fukuoka, Japan) for editing a draft of this manuscript.

Conflict of Interest

The authors declare no conflict of interest.

References

Bray, F., Laversanne, M., Sung, H., Ferlay, J., Siegel, R.L., Soerjomataram, I. & Jemal, A. (2024) Global cancer statistics 2022: GLOBOCAN estimates of incidence and mortality worldwide for 36 cancers in 185 countries. *CA Cancer J. Clin.*, **74**, 229-263.

Brierley, J.D., Gospodarowicz, M.K. & Wittekind, C. (2017) *TNM Classification of Malignant Tumours, 8th ed.*, Wiley-Blackwell, Hoboken, NJ.

DiNatale, A., Worrede, A., Iqbal, W., Marchioli, M., Toth, A., Sjostrom, M., Zhu, X., Corey, E., Feng, F.Y., Zhou, W. & Fatatis, A. (2022) IL-1beta expression driven by androgen receptor absence or inactivation promotes prostate cancer bone metastasis. *Cancer Res Commun*, **2**, 1545-1557.

Dwivedi, S., Goel, A., Natu, S.M., Mandhani, A., Khattri, S. & Pant, K.K. (2011) Diagnostic and prognostic significance of prostate specific antigen and serum interleukin 18 and 10 in patients with locally advanced prostate cancer: a prospective study. *Asian Pac. J. Cancer Prev.*, **12**, 1843-1848.

Guo, B., Fu, S., Zhang, J., Liu, B. & Li, Z. (2016) Targeting inflammasome/IL-1 pathways for cancer immunotherapy. *Sci. Rep.*, **6**, 36107.

Hamarsheh, S. & Zeiser, R. (2020) NLRP3 Inflammasome Activation in Cancer: A Double-Edged Sword. *Front. Immunol.*, **11**, 1444.

Karan, D., Tawfik, O. & Dubey, S. (2017) Expression analysis of inflammasome sensors and implication of NLRP12 inflammasome in prostate cancer. *Sci. Rep.*, **7**, 4378.

Merriel, S.W.D., Funston, G. & Hamilton, W. (2018) Prostate Cancer in Primary Care. *Adv. Ther.*, **35**, 1285-1294.

Miyauchi, T., Takahashi, M., Mitsuzuka, K., Saiki, Y., Okubo, T., Vertino, P.M., Goto, A., Arai, Y., Horii, A. & Fukushige, S. (2021) Aberrant Hypermethylation-Mediated Suppression of PYCARD Is Extremely Frequent in Prostate Cancer with Gleason Score >/= 7. *Dis. Markers*, **2021**, 8858905.

Moossavi, M., Parsamanesh, N., Bahrami, A., Atkin, S.L. & Sahebkar, A. (2018) Role of the NLRP3 inflammasome in cancer. *Mol. Cancer*, **17**, 158.

Narita, S., Nara, T., Kanda, S., Numakura, K., Saito, M., Inoue, T., Satoh, S., Nanjo, H., Tsuchiya, N., Mitsuzuka, K., Koie, T., Kawamura, S., Ohyama, C., Tochigi, T., Arai, Y. & Habuchi, T. (2019) Radical Prostatectomy With and Without Neoadjuvant Chemohormonal Pretreatment for High-Risk Localized Prostate Cancer: A Comparative Propensity Score Matched Analysis. *Clin. Genitourin. Cancer*, **17**, e113-e122.

Pierorazio, P.M., Walsh, P.C., Partin, A.W. & Epstein, J.I. (2013) Prognostic Gleason grade grouping: data based on the modified Gleason scoring system. *BJU Int.*, **111**, 753-760.

Sekhoacha, M., Riet, K., Motloung, P., Gumenku, L., Adegoke, A. & Mashele, S. (2022) Prostate Cancer Review: Genetics, Diagnosis, Treatment Options, and Alternative Approaches. *Molecules*, **27**.

Shahriari, K., Shen, F., Worrede-Mahdi, A., Liu, Q., Gong, Y., Garcia, F.U. & Fatatis, A. (2017) Cooperation among heterogeneous prostate cancer cells in the bone metastatic niche. *Oncogene*, **36**, 2846-2856.

Shao, X., Lei, Z. & Zhou, C. (2020) NLRP3 Promotes Colorectal Cancer Cell Proliferation and Metastasis via Regulating Epithelial Mesenchymal Transformation. *Anticancer Agents Med. Chem.*, **20**, 820-827.

Shi, F., Wei, B., Lan, T., Xiao, Y., Quan, X., Chen, J., Zhao, C. & Gao, J. (2021) Low NLRP3 expression predicts a better prognosis of colorectal cancer. *Biosci. Rep.*, **41**.

Stone, A.R., Bobo, W., Brat, D.J., Devi, N.S., Van Meir, E.G. & Vertino, P.M. (2004) Aberrant methylation and down-regulation of TMS1/ASC in human glioblastoma. *Am. J. Pathol.*, **165**, 1151-1161.

van Leenders, G., van der Kwast, T.H., Grignon, D.J., Evans, A.J., Kristiansen, G., Kweldam, C.F., Litjens, G., McKenney, J.K., Melamed, J., Mottet, N., Paner, G.P., Samaratunga, H., Schoots, I.G., Simko, J.P., Tsuzuki, T., et al. (2020) The 2019 International Society of Urological Pathology (ISUP) Consensus Conference on Grading of Prostatic Carcinoma. *Am. J. Surg. Pathol.*, **44**, e87-e99.

Wang, H., Luo, Q., Feng, X., Zhang, R., Li, J. & Chen, F. (2018) NLRP3 promotes tumor growth and metastasis in human oral squamous cell carcinoma. *BMC Cancer*, **18**, 500.

Wang, H., Wang, Y., Du, Q., Lu, P., Fan, H., Lu, J. & Hu, R. (2016a) Inflammasome-independent NLRP3 is required for epithelial-mesenchymal transition in colon cancer cells. *Exp. Cell Res.*, **342**, 184-192.

Wang, Y., Kong, H., Zeng, X., Liu, W., Wang, Z., Yan, X., Wang, H. & Xie, W. (2016b) Activation of NLRP3 inflammasome enhances the proliferation and migration of A549 lung cancer cells. *Oncol. Rep.*, **35**, 2053-2064.

Xu, Z., Wang, H., Qin, Z., Zhao, F., Zhou, L., Xu, L. & Jia, R. (2021) NLRP3 inflammasome promoted the malignant progression of prostate cancer via the activation of caspase-1. *Cell Death Discov*, **7**, 399.

Xue, Y., Du, H.D., Tang, D., Zhang, D., Zhou, J., Zhai, C.W., Yuan, C.C., Hsueh, C.Y., Li, S.J., Heng, Y., Tao, L. & Lu, L.M. (2019) Correlation Between the NLRP3 Inflammasome and the Prognosis of Patients With LSCC. *Front. Oncol.*, **9**, 588.

Zheng, L. & Liu, H. (2022) Prognostic association between NLRP3 inflammasome expression level and operable pancreatic adenocarcinoma. *Int. J. Biol. Markers*, **37**, 314-321.

Supplementary Files

Please find supplementary file(s);
https://doi.org/10.1620/tjem.2024.J074